

Electronic Structure of Cobalt Carbide, CoC

Demeter Tzeli and Aristides Mavridis*

Laboratory of Physical Chemistry, Department of Chemistry, National and Kapodistrian University of Athens, P.O. Box 64 004, 157 10 Zografou, Athens, Greece

Received: April 17, 2006; In Final Form: May 22, 2006

The ground and 18 low lying excited states of the diatomic molecule cobalt carbide, CoC, have been examined by multireference variational methods (MRCI) combined with quantitative basis sets. All calculated states are bound and correlate adiabatically to the ground-state atoms, Co(a^4F) + C(3P). We report complete potential energy curves, equilibrium bond distances, dissociation energies (D_e), spectroscopic constants, electric dipole moments and spin–orbit splittings. The bonding character of certain states is also discussed with the help of Mulliken distributions and valence-bond-Lewis diagrams. We are practically certain that the ground state is of $^2\Sigma^+$ symmetry with a state of $^2\Delta$ symmetry lying less than 3 kcal/mol higher, in agreement with the relevant experimental findings. Our best estimate of the X $^2\Sigma^+$ dissociation energy is $D_e(D_0) = 83(82)$ kcal/mol at $r_e = 1.541$ Å, 0.02 Å shorter than the experimental bond length.

1. Introduction

The diatomic 3d-transition metal carbides MC, M = Sc–Cu, are clearly of paramount importance for both practical and academic reasons: practical, because M–C bonds are encountered in a plethora of interesting materials, and academic, because the character of the M–C bond does not comply to the conventional “chemical wisdom” about bonding. The reasons for this bonding unorthodoxy have been discussed in our previous publications on ScC,^{1a} TiC,^{1b} VC,^{1c} CrC,^{1d} MnC,^{1e} and FeC;^{1f,g} work in this laboratory is also in progress on NiC and CuC carbides. The vagaries of the 3d-transition metal containing diatomics are described as well in the excellent review article by Harrison.²

Henceforth, we present high level multireference variational ab initio calculations on the ground (X) and eighteen (18) excited states (doublets, quartets and sextets) of cobalt carbide, CoC. To the best of our knowledge there are four experimental^{3–6} and two theoretical^{7,8} studies on CoC.

In 1986, van Zee et al.³ obtained the ESR spectrum of the CoC radical, and concluded that its lowest state should be of $^2\Sigma$ symmetry. These workers also referred to a $^2\Pi_i$ state interacting strongly with the $^2\Sigma$ and located approximately 66 kcal/mol higher. About 10 years later, Barnes et al.⁴ measured the laser-induced fluorescence rotational spectrum of jet-cooled CoC near 750 nm. It was established that the ground state is of $^2\Sigma^+$ symmetry with a low lying $^2\Delta_{5/2}$ state just 221 cm^{-1} higher; its $^2\Delta_{3/2}$ companion is reported to be 1173 cm^{-1} above the X-state, i.e., $\Delta E(^2\Delta_{3/2} \leftarrow ^2\Delta_{5/2}) = 952$ cm^{-1} . The equilibrium bond lengths and harmonic frequencies of the X $^2\Sigma^+$ and $^2\Delta_{5/2}$ states are $r_0 = 1.5612, 1.6424$ Å and $\omega_e = 934, 838$ cm^{-1} , respectively.⁴ They also reported experimental results for three other states ($^2\Sigma^+, ^2\Pi$, and $\Omega' = 3/2$). Barnes et al. concluded their work by saying: “Various excited states have been observed near 750 nm. Among these are what appears to be a heavily perturbed $^2\Pi_i$ state; its exact nature is unclear and must await detailed ab initio calculations”.⁴ We will try to shed some light on this $^2\Pi_i$ state, the same one that van Zee and co-workers were referring to 10 years earlier.³

In 1997 Adam et Peers⁵ through laser-induced fluorescence studies, reported the rotational analysis of the CoC [14.0] $^2\Sigma^+ - X$ $^2\Sigma^+$ transition. For the X $^2\Sigma^+$ and [14.0] $^2\Sigma^+$ states they obtained $r_0 = 1.5612$ ($r_e = 1.5601$) Å and $r_e = 1.747$ Å, respectively, with $\Delta E([14.0] ^2\Sigma^+ \leftarrow X ^2\Sigma^+) = 14243$ cm^{-1} (=40.723 kcal/mol). Adam and Peers close their paper by saying that: “Detailed ab initio calculations on excited states would greatly assist in the further interpretation of these data.”⁵

Finally, in 2001, Brewster and Ziurys⁶ recorded the pure rotational spectrum of the CoC X $^2\Sigma^+$ state. The equilibrium bond length determined (r_0) was found to be in complete agreement with the results of the previous two optical experimental studies.^{4,5}

On the theoretical side now, Gutsev et al.⁷ studied the ground states of MC^{0,±} carbides (M = Sc–Zn) by density functional theory (DFT); for the entire MC series they report r_e , ω_e , dipole moments (μ), binding energies (D_0), diabatic electron affinities and ionization energies.

Very recently Borin et al.⁸ published the first ab initio study on CoC, using the multistate multiconfigurational second-order perturbation theory (MS-CASPT2) of Roos and co-workers,⁹ coupled with a newly developed atomic natural orbital basis sets by the same group.¹⁰ These basis sets include scalar relativistic effects obtained through the Douglas–Kroll–Hess (DKH) approach, plus specially tuned functions to account for the $3s^2 3p^6$ semicore correlation of the metal atom(s). Specifically, the basis set used in this study is (21s15p10d6f4g2h/_{Co} 14s9p4d3f/_C) contracted to [7s6p4d3f2g/_{Co} 5s4p3d2f/_C]. Borin et al.⁸ calculated the first seven doublets (X $^2\Sigma^+$, A $^2\Delta$, B $^2\Phi$, C $^2\Phi$, D $^2\Pi$, E $^2\Pi$, [14.0] $^2\Sigma^+$), reporting partial (up to Co–C distances of 2.1 Å) potential energy curves, equilibrium bond lengths, dissociation energies, harmonic frequencies and energy separations. As we will see, their results deviate considerably from the ones obtained here.

In the present work we have performed high level multireference and coupled-cluster (for the two lowest states) calculations in conjunction with large basis sets. For the eight doublets, seven quartets, and four sextets, we report complete

potential energy curves (PEC), energetics, common spectroscopic parameters, and dipole moments; the deciphering of the Co–C bond is also one of the goals of the present study.

In section 2 we define the technical approach followed, in section 3 our results are discussed, and in section 4 some final remarks and comments are presented.

2. Computational Approach

For the Co atom the averaged atomic natural orbital (ANO) basis set of Bauschlicher,¹¹ (20s15p10d6f4g), and for the C atom the correlation consistent basis set of quadruple cardinality by Dunning,¹² cc-pVQZ = (12s6p3d2f1g) were used. Both sets were generally contracted to [7s6p4d3f2g/c_o 5s4p3d2f1g/c], thus containing 139 spherical Gaussian functions. For the two lowest CoC states (²Σ⁺, ²Δ) the recently developed extended correlation consistent basis sets of quadruple quality by Balabanov and Peterson¹³ for the 3d-transition metal elements, cc-pVQZ = 22s18p11d3f2g1h, combined with the cc-pVQZ of Dunning¹² for the C atom were employed, generally contracted to [8s7p5d3f2g1h/c_o 5s4p3d2f1g/c] ≡ 4Z. Finally, to account for the 3s²3p⁶ core-valence correlation effects, the cobalt-pVQZ set was augmented by a series of 2s + 2p + 2d + 1f + 1g + 1h weighted core functions, as suggested in ref 13. Combining with the cc-pVQZ basis set of C gives rise to the contracted [10s9p7d4f3g2h/c_o 5s4p3d2f1g/c] ≡ C4Z set, spanning a 204 dimensional one-electron space.

The inherent multireference character of CoC and our desire to construct complete potential energy curves (PEC), makes the use of a multireference approach compulsory. Hence, the complete active space self-consistent field + single + double replacements (CASSCF + 1 + 2 = MRCI) methodology was used for all states studied. For the two lowest states (²Σ⁺, ²Δ) the restricted coupled cluster + singles + doubles + perturbative triples (RCCSD(T)) single reference method was also tried, but using CASSCF natural orbitals.

The multireference zeroth-order functions were built by allocating the 13 active electrons (3d⁷4s² on Co + 2s²2p² on C) to a 10 valence orbital space (one 4s and five 3d on Co + one 2s and three 2p on C). The size of our reference spaces range from 474 (⁶Δ) to 3526 (²Σ⁺) configuration functions (CF), with CI spaces ranging from 49 × 10⁶ (²Π) to 134 × 10⁶ (²Σ⁺) CFs. When the internal contraction (icMRCI) scheme of Werner and Knowles is applied,¹⁴ the CI expansions are reduced by about 2 orders of magnitude (~2.45 × 10⁴ to 1.22 × 10⁶). The estimation of core-correlation effects (core ≡ 3s²3p⁶ of Co) in the two lowest states was obtained by including the 8 semicore electrons of Co in the CI procedure; these calculations will be referred to as C-MRCI. For the Balabanov–Peterson basis set the C-MRCI (icC-MRCI) expansions contain about 1.7 × 10⁹ (20 × 10⁶) CFs. Scalar relativistic effects for the two lowest ²Σ⁺ and ²Δ states were estimated through the second-order Douglas–Kroll–Hess^{15,16} (DKH2) approximation. For the 1 ²Δ, 2 ⁴Φ, 3 ⁴Π, 4 ²Φ, 5 ²Φ, 6 ²Π, 7 ⁴Δ, and 8 ²Π states the spin-orbit (SO) splittings were calculated using the previous uncontracted basis sets of Bauschlicher and Dunning (but with the g functions removed) at the MRCI/(20s15p10d6f/c_o 12s6p3d2f/c) level of theory through the Breit–Pauli operator.

With the counterpoise technique,¹⁷ the basis set superposition errors (BSSE) of the X ²Σ⁺ and 1 ²Δ states at the MRCI level were determined to be 0.63 and 0.57 kcal/mol by employing the Bauschlicher (B) basis set on Co.¹¹ The corresponding values of the Balabanov–Peterson (P) basis (4Z)¹³ are 0.65 and 0.60 kcal/mol, respectively.

All calculations were done under C_{2v} symmetry constraints, whereas the CASSCF wave functions were enforced to possess

TABLE 1: Total Energies (hartree) of the a⁴F(4s²3d⁷) and b⁴F(4s¹3d⁸) States, and the b⁴F ← a⁴F Energy Separation (eV) of Co at Different Levels of Theory

method ^d	Co		
	a ⁴ F	b ⁴ F	b ⁴ F ← a ⁴ F
MRCI ^b	−1381.67029	−1381.65300	0.470
MRCI ^c	−1381.67398	−1381.65669	0.471
MRCI+Q ^b	−1381.6886	−1381.6706	0.489
MRCI+Q ^c	−1381.6923	−1381.6740	0.498
MRCI+DKH2 ^b	−1392.12073	−1392.09172	0.789
MRCI+DKH2 ^c	−1392.11863	−1392.08972	0.787
MRCI+DKH2+Q ^b	−1392.1397	−1392.1102	0.801
MRCI+DKH2+Q ^c	−1392.1373	−1392.1076	0.809
C-MRCI ^b	−1382.00557	−1382.99261	0.353
C-MRCI ^c	−1382.08937	−1382.07717	0.329
C-MRCI+Q ^b	−1382.0503	−1382.0390	0.308
C-MRCI+Q ^c	−1382.1382	−1382.1276	0.284
C-MRCI+DKH2 ^b	−1392.51129	−1392.48591	0.691
C-MRCI+DKH2 ^c	−1392.53485	−1392.51081	0.654
C-MRCI+DKH2+Q ^b	−1392.5597	−1392.5363	0.638
C-MRCI+DKH2+Q ^c	−1392.5844	−1392.5620	0.609
expt ^d			0.417

^a Q and DKH2 refer to the Davidson correction and to second-order Douglas–Kroll–Hess scalar relativistic corrections. ^b Bauschlicher’s basis set for Co, [7s6p4d3f2g]. ^c Peterson’s basis sets for Co, [8s7p5d3f2g1h] and [10s9p7d4f3g2h] for the C-calculations. ^d Reference 21.

axial angular momentum symmetry, i.e., |Λ| = 0 (Σ), 1 (Π), 2 (Δ) and 3 (Φ). For the excited states 5 ²Φ, 8 ²Π, 10 ²Σ⁺, 11 ²Δ, 12 ⁴Δ, 15 ⁴Π, and 16 ⁴Φ the state average (SA) approach¹⁸ was used due to their strong interaction with states of the same symmetry species.

Finally, it should be mentioned that because of the relatively large number of active electrons (13), the MRCI, and of course more so the C-MRCI calculations, suffer from significant size nonextensivity errors: 11 mh at the MRCI, minimized to about 3 mh after including the Davidson correction¹⁹ for unlinked clusters (+Q) and approximately the same for all studied states.

All calculations were performed with the MOLPRO 2002.6 suite of codes.²⁰

3. Results and Discussion

Table 1 records absolute energies of the first two states of the Co atom, a⁴F(4s²3d⁷) and b⁴F(4s¹3d⁸), along with the b⁴F ← a⁴F energy separation at different levels of theory. Observe that at the MRCI level and in both basis sets ((B)auschlicher¹¹ or (P)eterson¹³), the calculated atomic splitting b⁴F ← a⁴F is in fair agreement with the experimental value, 0.470 vs 0.417 eV.²¹ However, by increasing the sophistication of the method from MRCI to C-MRCI + DKH2 + Q, the theoretical results depart monotonically from the experimental value. Obviously, the good MRCI agreement is rather fortuitous due to cancellation of errors.

The ground states of Co(a⁴F) and C(³P) give rise to a total of 36 molecular CoC ^{2S+1}Λ states, namely, ^{2S+1}(Γ[1], Φ[2], Δ[3], Π[3], Σ[3]) with 2S + 1 = 2, 4, and 6, out of which the first nineteen have been investigated as indicated by preliminary CASSCF calculations.

Numerical results of the first two lower states ²Σ⁺ and ²Δ in a variety of methods, and of the remaining seventeen states limited to the MRCI or MRCI+Q/[7s6p4d3f2g/c_o 5s4p3d2f1g/c] level, are listed in Table 2. For all 19 states Table 3 catalogues leading MRCI configurations and atomic Mulliken populations, valence-bond-Lewis (vbL) diagrams indicating graphically the bonding character of every state, and asymptotic fragments. Figure 1 depicts a relative level diagram of the states studied

TABLE 2: (Continued)

state	methods ^a	$-E$	r_e	D_e	ω_e	$\omega_e x_e$	$10^{-3}\alpha_e$	$10^{-7}\bar{D}_e$	q_{Co}	$\langle\mu\rangle^b$	μ_{FF}^b	T_e
$8^2\Pi$	MRCI	1419.51524	1.665	45.8	1130.7	49.4	3.95	0.718	0.20	1.59	2.61	35.7
	MRCI+Q	1419.5540	1.655	51.3							2.74	33.6
	CASPT2+DKH ^f		1.642	75.4	949							35.41
$9^4\Sigma^+$	CASSCF	1419.16316	2.046	24.7	501.1	4.05	2.72	1.05	0.48	3.03	3.03	16.3
	MRCI	1419.50573	1.755	38.7	451	63			0.32	1.58	2.18	41.7
	MRCI+Q	1419.5401	1.698	41.9							2.67	42.3
$10^2\Sigma^+$	MRCI	1419.50064	1.764	36.7	721	2.8			0.22	1.40	2.34	44.9
	MRCI+Q	1419.5385	1.745	41.6							2.44	43.3
	CASPT2+DKH ^f		1.676	73.1	1252							37.67
	expt ^h		~ 1.80		685							39.89
$11^2\Delta$	expt ⁱ		1.747		617		5.31					40.72
	MRCI	1419.49971	1.726	36.2	716				0.17	0.082	0.68	45.5
	MRCI+Q	1419.5349	1.709	39.4							0.81	45.6
$\Omega' = 3/2$	expt ^h		1.75		643							38.39
	MRCI	1419.49962	1.776	36.0	904.0	13.0	4.36	7.56	0.24	1.19	1.67	45.6
$12^4\Delta$	MRCI+Q	1419.5349	1.763	39.4							1.63	45.5
	CASSCF	1419.16320	2.048	25.4	525.0	3.44	3.12	9.50	0.47	2.68	2.68	16.2
$13^6\Phi$	MRCI	1419.49911	1.953	35.0	496.4	3.29	2.10	1.41	0.40	2.15	2.23	45.9
	MRCI+Q	1419.5284	1.933	34.9							2.59	49.7
	CASSCF	1419.15865	2.064	21.9	515.6	4.10	3.34	9.40	0.48	2.95	2.95	19.1
$14^6\Sigma^+_G{}^k$	MRCI	1419.49496	1.975	31.9	473.5	9.97	-1.05	1.46	0.41	2.55	3.06	48.5
	MRCI+Q	1419.5246	1.954	32.1							3.08	52.0
	MRCI	1419.49301	1.694	30.7	979	10.4			0.34	2.58	3.85	49.7
$14^6\Sigma^+_L{}^k$	MRCI+Q	1419.5290	1.676	34.9							3.92	49.3
	MRCI	1419.49391	1.780	32.4	824.0	13.2	7.32	8.80	0.26	1.86	3.00	49.1
$15^4\Pi$	MRCI+Q	1419.5306	1.760	36.6							3.00	48.3
	MRCI	1419.49353	1.826	32.3	767.4	18.8	3.49	8.87	0.28	1.89	2.81	49.4
$16^4\Phi$	MRCI+Q	1419.5276	1.809	34.9							2.92	50.2
	CASSCF	1419.15650	2.067	21.7	507.8	3.66	3.23	0.962	0.47	2.82	2.82	20.4
$17^6\Pi$	MRCI	1419.49249	1.987	31.1	483.5	3.09	2.18	1.35	0.40	2.36	2.72	50.0
	MRCI+Q	1419.5220	1.975	31.0							2.68	53.7
	CASSCF	1419.15730	2.073	21.1	497.6	3.37	3.26	0.983	0.47	2.64	2.64	19.9
$18^6\Delta$	MRCI	1419.49127	2.003	29.5	477.0	2.36	3.07	1.31	0.40	2.15	2.39	50.8
	MRCI+Q	1419.5203	1.997	29.4							2.32	54.7

^a Q and DKH2 refer to Davidson and to second-order Douglas–Kroll–Hess relativistic corrections. ^b $\langle\mu\rangle$ calculated as expectation value, μ_{FF} by the finite field method. ^c Numbers in parentheses are calculated using the Peterson's basis set cc-pVQZ. ^d Semicore $3s^23p^6$ electrons of the Co atom included in the CI. ^e Reference 7. ^f Reference 8. ^g The energy value is estimated from Figure 1 of ref 8. ^h Reference 4, r_0 value. ⁱ Reference 5. ^j Reference 6, r_0 value. ^k G and L refer to global and local minima.

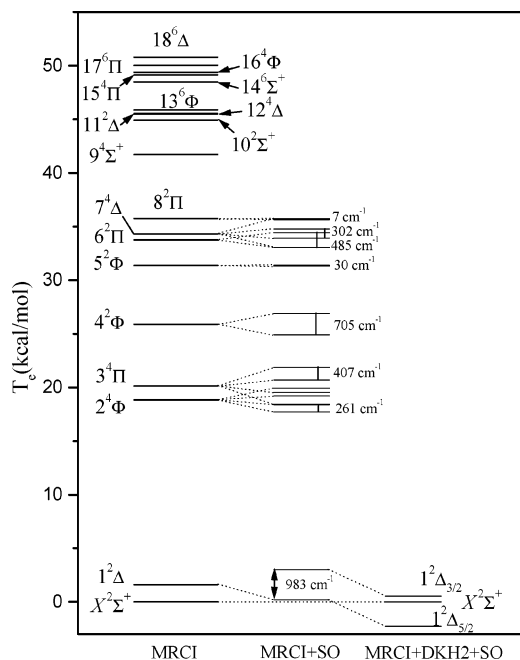


Figure 1. MRCI relative energy levels of CoC including SO splittings.

along with SO-splittings of the $1^2\Delta$, $2^4\Phi$, $3^4\Pi$, $4^2\Phi$, $5^2\Phi$, $6^2\Pi$, $7^4\Delta$, and $8^2\Pi$ states, and Figure 2 displays the totality of PECs studied. Each excited state has been labeled with a serial number in front of the symmetry symbol revealing its absolute energy order with respect to the ground (X) state.

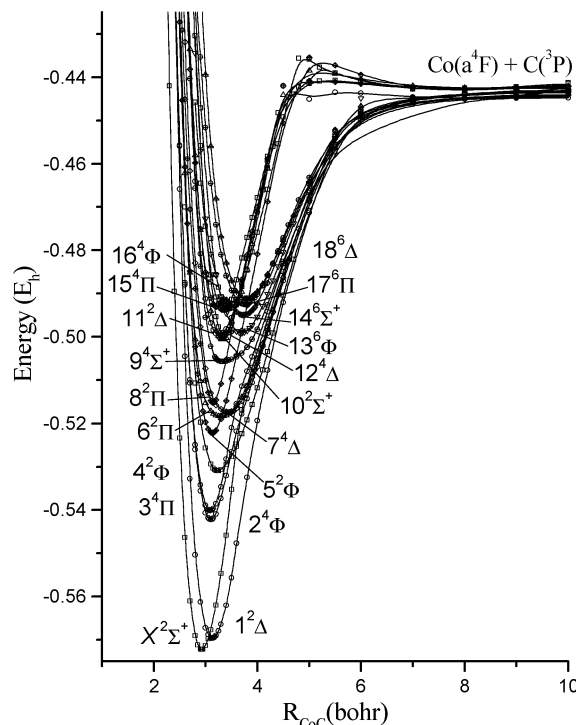


Figure 2. Potential energy curves of 19 states of CoC at the MRCI/[7s6p4d3f2g/co 5s4p3d2f1g/c] level of theory.

Finally, Figures 3–5 present separately the PECs according to their spin multiplicity. Note that all states correlate to the ground-state atoms, $Co(a^4F) + C(^3P)$.

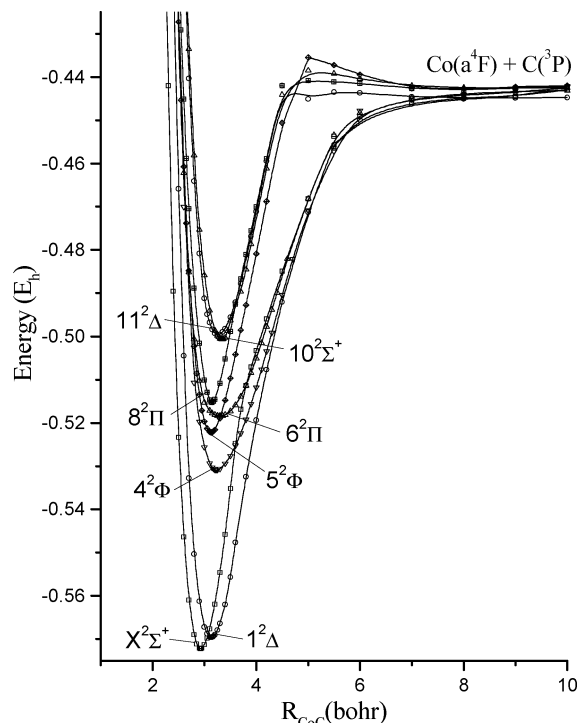


Figure 3. MRCI potential energy curves of the CoC doublets.

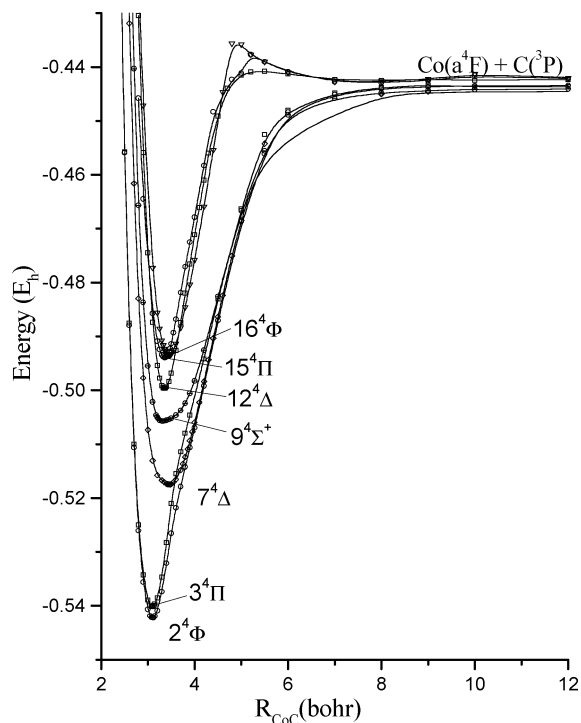


Figure 4. MRCI potential energy curves of the CoC quartets.

In what follows we examine first the doublets, then the quartets and finally the sextets.

A. Doublets: $X^2\Sigma^+$, $1^2\Delta$, $4^2\Phi$, $5^2\Phi$, $6^2\Pi$, $8^2\Pi$, $10^2\Sigma^+$, and $11^2\Delta$. Experimentally, the ground state of CoC is of $^2\Sigma^+$ symmetry,^{3–6} and the same could be said theoretically but not without some reservations (see below). According to Table 3 the asymptotic wave function can be described by the product $|a^4F; M=0\rangle_{Co} \times |^3P; M=0\rangle_C$. As the two atoms come closer, an avoided crossing occurs around 3.8 bohr with the $10^2\Sigma^+$ state. However, the latter had already suffered an avoided crossing with an incoming (not calculated) $^2\Sigma^+$ state correlating

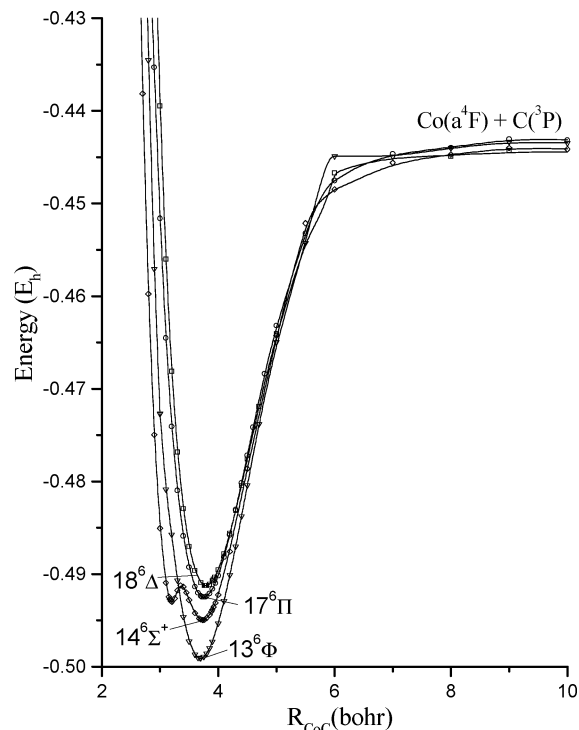


Figure 5. MRCI potential energy curves of the CoC sextets.

to the b^4F state of the Co atom. As a result, the equilibrium atomic character of the $X^2\Sigma^+$ is $Co(b^4F, s^1d^8; M=0) + C(^3P; M=0)$. The atomic Mulliken populations and the leading configuration point clearly to a triple $2\pi + \sigma$ bond between the Co and C atoms, as shown in the vbL diagram of Table 3. About $0.5 e^-$ are transferred from the $\sim 4p3d_z^2$ Co hybrid to the empty $2p_z$ orbital of the C atom ($M=0$), with $0.4 e^-$ leaking back to the metal through the π_x, π_y system.

Table 2 lists total energies, spectroscopic parameters and dipole moments of the $X^2\Sigma^+$ and $1^2\Delta$ states obtained at the multireference and coupled-cluster methods. Notice that at the MRCI, MRCI+Q, MRCI+DKH2, and MRCI+DKH2+Q levels of theory, all our results are almost identical in both B and P basis sets. Moving to C-level, i.e., including the $3s^23p^6$ electrons of Co in the CI procedure, only slight differences are observed between the B and P bases in all properties studied. At the highest level of theory, namely, C-MRCI+DKH2+Q+BSSE/C4Z, $D_e(D_0) = 83(82)$ kcal/mol with respect to the ground-state atoms, and $r_e = 1.541 \text{ \AA}$, 0.02 \AA shorter than the experimental one.^{4–6} It is interesting that exactly the same D_e value is obtained at the “simple” valence MRCI+Q and RCCSD(T) levels with $r_e = 1.550$ and 1.541 \AA , respectively. We recall that the D_e values of all triple bonded MC carbides, that is VC($X^2\Delta$),^{1c} CrC($X^3\Sigma^-$),^{1d} MnC($X^4\Sigma^-$),^{1e} FeC($X^3\Delta$),^{1f,g} and NiC($X^1\Sigma^+$)²² obtained at about the same level of theory as the present one, are 95, 89, 70, 90, and 87 kcal/mol, respectively, in conformity with the D_e value of the $X^2\Sigma^+$ state of CoC. Corresponding experimental results for the ground states of VC,²³ FeC,²⁴ and NiC²⁵ are 100.1 ± 5.7 , 91.2 ± 7 , and larger than 78.2 kcal/mol, respectively; no experimental results are available for the CrC and MnC carbides. Hence, we believe that the reported dissociation energy of $D_e = 111$ kcal/mol by Borin et al.,⁸ is rather overestimated by about 25–30 kcal/mol.

The next state is of $^2\Delta$ symmetry, correlates to $Co(a^4F; M=\pm 2) + C(^3P; M=0)$, and suffers an avoided crossing around 4 bohr with the $11^2\Delta$ state. Thus its in situ equilibrium atoms switch to $Co(a^4F; M=\pm 3) + C(^3P; M=\mp 1)$, and it is

genuinely triple bonded with a slightly negative carbon atom ($\sim 0.2 e^-$). Although we have tagged the ground state as $^2\Sigma^+$ following the experimentalists, our calculations indicate that a $^2\Delta$ symmetry is a strong contender for being the lowest state; it is interesting to follow the results of Table 2. At the valence MRCI(+Q) level, $T_e(^2\Delta \leftarrow ^2\Sigma^+) = 1.62(0.2)$ kcal/mol, but the picture changes by adding the scalar relativistic effects, namely, $T_e(^2\Delta \leftarrow ^2\Sigma^+) = -1.92(-3.3)$ kcal/mol, the $^2\Delta$ state becoming now the lowest. At the C-MRCI(+Q)/C4Z level, $T_e(^2\Delta \leftarrow ^2\Sigma^+) = 3.12(1.9)$ kcal/mol. However, at the highest level of calculation, C-MRCI+DKH2(+Q)/C4Z, $T_e = -0.39(-1.6)$ kcal/mol, i.e., the $^2\Delta$ state is lower than the $^2\Sigma^+$ by about 1.6 kcal/mol.

Experimentally, the $^2\Delta_{5/2}$ and $^2\Delta_{3/2}$ states are 221 and 1173 cm^{-1} above the $^2\Sigma^+$ state,⁴ with the mean value 697 cm^{-1} ($=1.99$ kcal/mol) higher. This number is in excellent agreement with the valence MRCI and C-MRCI+Q/C4Z results of the present work, which predict that $T_e(^2\Delta \leftarrow ^2\Sigma^+) = 1.62$ and 1.9 kcal/mol, respectively; it is the addition of the scalar relativistic effects that inverts the two states, suggesting that the $^2\Delta$ is lower by 1.6 kcal/mol with respect to $^2\Sigma^+$. Recall, however, that the $^2\Sigma^+$ state correlates *adiabatically* to the first excited $b^4F(4s^13d^8)$ state of Co, whereas the $^2\Delta$ to the $a^4F(4s^23d^7)$. The C-MRCI+DKH2+Q/C4Z $b^4F \leftarrow a^4F$ energy separation is 0.609 eV (Table 1), 0.192 eV *higher* than the experimental one, and this large error is the cause of predicting the $^2\Delta$ state lower than the $^2\Sigma^+$ at this level of theory. By parallel downshifting of the $^2\Sigma^+$ PEC by 0.192 eV $= 4.43$ kcal/mol, the $^2\Sigma^+$ becomes the ground state, lying approximately $4.4 - 1.6 = 2.8$ kcal/mol lower than the $^2\Delta$, and in fair agreement now with experiment. Therefore, it seems rather certain that the ground state of CoC is of $^2\Sigma^+$ symmetry.

Finally, we report that the MRCI/(20s15p10d6f/c_o 12s6p3d2f/c) $^2\Delta_{3/2} - ^2\Delta_{5/2}$ SO-splitting is calculated to be 989 cm^{-1} , in rather good agreement with the experimental⁴ value of 952 cm^{-1} .

The next two doublets $4^2\Phi$ and $5^2\Phi$ are of intense multireference character; they are double bonded (σ, π) and correlate to $\text{Co}(a^4F; M = \pm 3, \pm 2) + \text{C}(^3P; M = 0, \pm 1)$, respectively (Table 3). An avoided crossing at 5.0 bohr of $5^2\Phi$ with another (not calculated) $^2\Phi$ state correlating to the b^4F atomic state of Co, transforms its character to $\text{Co}(b^4F; M = \pm 3) + \text{C}(^3P; M = 0)$; the strong interaction of the $5^2\Phi$ and $4^2\Phi$ states, which follows around equilibrium (~ 3 bohr), increases the complexity of these two $^2\Phi$ states.

Their MRCI(+Q) D_e and r_e values are 54.9(58.1), 50.3(54.5) kcal/mol and 1.713(1.682), 1.657(1.652) Å, respectively. The MRCI/(20s15p10d6f/c_o 12s6p3d2f/c) SO splittings of $4^2\Phi$ and $5^2\Phi$ states are $\Delta E(^2\Phi_{7/2} - ^2\Phi_{5/2}) = 705$ and 30 cm^{-1} , respectively; Figure 1. The results of Borin et al.⁸ differ significantly from ours, most notably in the dissociation energies. It is curious that the D_e values of all seven doublets calculated in ref 8 are systematically larger than the corresponding ones calculated presently by about 30 kcal/mol; see Table 2.

Two $^2\Pi$ states, almost degenerate, marked $6^2\Pi$ and $8^2\Pi$, have been obtained at the MRCI(+Q) level of theory with energy distances from the X $^2\Sigma^+$ state of 33.7(34.0) and 35.7-(33.6) kcal/mol, respectively. Both are of intense multireference nature, double bonded (σ, π) and correlating to $\text{Co}(a^4F; M = \pm 1, \pm 2) + \text{C}(^3P; M = 0, 1)$. The $8^2\Pi$ suffers two avoided crossings around 6.5 and 5.0 bohr with a higher (not calculated) $^2\Pi$ state. Passing the equilibrium of the $6^2\Pi$ state, $r_e = 1.745$ Å ($=3.30$ bohr), the $8^2\Pi$ suffers a third avoided crossing now with the $6^2\Pi$ state, very close to its equilibrium geometry, $r_e = 3.13$ bohr. The MRCI SO splittings of the 6 and $8^2\Pi$ states, are $\Delta E(^2\Pi_{3/2} - ^2\Pi_{1/2}) = 485$ and 7 cm^{-1} , respectively; Figure 1. Experimentally,⁴ two transitions at 13343 and 13079 cm^{-1}

have been observed, which probably correspond to the $v = 0$ SO components of the $^2\Pi_i$ state, with $\Delta E(^2\Pi_{3/2} - ^2\Pi_{1/2}) = 264$ cm^{-1} . Because the 6 and $8^2\Pi$ states are practically degenerate at the MRCI+Q level, we cannot tell with certainty to which one the experimentally determined $^2\Pi_i$ state corresponds. Perhaps, the two X- $^2\Pi_i$ transitions that the experimentalists see are not the $3/2$ and $1/2$ components of one $^2\Pi$ state, but belong to the two $^2\Pi$ degenerate states, i.e., ($8^2\Pi_{1/2,3/2}, 6^2\Pi_{1/2}$) \leftarrow X $^2\Sigma^+$.

10 $^2\Sigma^+$. This is a triple bonded strongly multireference state correlating to $\text{Co}(a^4F; M = \pm 1) + \text{C}(^3P; M = \mp 1)$; see Table 3. There are two avoided crossings, one at 5 bohr with the higher excited state $^2\Sigma^+$ correlating to $\text{Co}(b^4F; M = 0) + \text{C}(^3P; M = 0)$, and then at 3.8 bohr with the ground state. As a result, the in situ equilibrium atoms are $\text{Co}(a^4F; M = 0) + \text{C}(^3P; M = 0)$. Experimentally, the $10^2\Sigma^+$ state is located 39.89⁴ or 40.72 kcal/mol⁵ (T_e) above the X state, with an r_e of 1.747 Å.⁵ Our MRCI(+Q) results are in acceptable agreement with these experimental findings, namely, $T_e = 44.9(43.3)$ kcal/mol and $r_e = 1.764(1.745)$ Å; Table 2.

11 $^2\Delta$. This is the highest of the doublets studied, double bonded (π, π), with $D_e = 36.2(39.4)$ kcal/mol, $T_e = 45.5(45.6)$ kcal/mol, and $r_e = 1.726(1.709)$ Å at the MRCI(+Q) level; see Tables 2 and 3. Experimentally, a state at $T_0 = 38.39$ kcal/mol⁴ and $r_0 = 1.75$ Å with a total angular momentum $\Omega' = 3/2$ has been observed, which could be the $3/2$ component of either a $^2\Pi$ or $^2\Delta$ state.

B. Quartets: 2 $^4\Phi$, 3 $^4\Pi$, 7 $^4\Delta$, 9 $^4\Sigma^+$, 12 $^4\Delta$, 15 $^4\Pi$, and 16 $^4\Phi$. The potential energy curves of the seven quartets studied in the present work are displayed in Figure 4; the MRCI/(20s15p10d6f/c_o 12s6p3d2f/c) SO-splittings of the $2^4\Phi$, $3^4\Pi$, and $7^4\Delta$ states are shown in Figure 1.

2 $^4\Phi$, 16 $^4\Phi$. Formally, the $2^4\Phi$ is the lowest of the quartets with a $^4\Pi$ state just 1.3(0.8) kcal/mol higher at the “simple” MRCI(+Q) level. Whereas both $^4\Phi$ correlate to the ground-state atoms $\text{Co}(a^4F; 4s^23d^7) + \text{C}(^3P)$, the $16^4\Phi$ experiences an avoided crossing around 4.6 bohr with a higher (not calculated) $^4\Phi$ correlating to the first excited state of $\text{Co}(b^4F; 4s^13d^8) + \text{C}(^3P)$. As we move closer to equilibrium, it seems that the $16^4\Phi$ state interacts with the $2^4\Phi$ at about 3.5 bohr; therefore, the in situ equilibrium character of Co atom in the latter acquires the $4s^13d^8$ distribution. The resulting double bond (σ, π) character in the $2^4\Phi$ state of CoC, along with Mulliken populations and leading configurations, are depicted in Table 3. The bonding in the $16^4\Phi$ state is also (σ, π), but now the in situ Co atom possesses a $4s^23d^7(a^4F)$ distribution; see the vBL diagram in Table 3. At the MRCI(+Q) level the $2^4\Phi$ and $16^4\Phi$ states are located 18.8(17.4) and 49.4(50.2) kcal/mol above the X state with binding energies with respect to $\text{Co}(a^4F) + \text{C}(^3P)$ of, $D_e = 62.0(67.2)$ and 32.3(34.9) kcal/mol, respectively (Table 2).

3 $^4\Pi$, 15 $^4\Pi$. Recall that under C_{2v} symmetry the Π and Φ states have the same spatial symmetry, i.e., B_1 . The $3^4\Pi$ is practically degenerate to $2^4\Phi$, and the $15^4\Pi$ to $16^4\Phi$. In all respects these two $^4\Pi$ states are strikingly similar to the two $^4\Phi$ states just discussed; see Tables 2 and 3.

7 $^4\Delta$, 12 $^4\Delta$. Both these quartets are double bonded, of (σ, π) character the $7^4\Delta$ and (π, π) the $12^4\Delta$ state; see Table 3. The $12^4\Delta$ suffers an avoided crossing around 4.5 bohr with an incoming (not calculated) $^4\Delta$ state correlating to $\text{Co}(b^4F; 4s^13d^8) + \text{C}(^3P)$, therefore imparting this character to the in situ equilibrium atoms of the $12^4\Delta$ state. An avoided crossing also occurs between the $7^4\Delta$ and $12^4\Delta$ states in the repulsive part of their potential energy curves (Figure 4).

TABLE 3: MRCI Leading Configurations, Mulliken Populations, Valence-Bond-Lewis Diagrams and M(Co), M(C) Projection Values of Asymptotic Atoms, Co(a^4F ; M) + C(3P ; M)

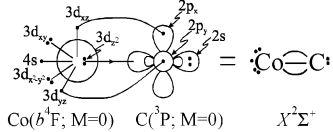
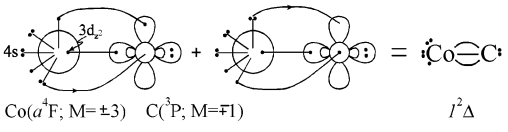
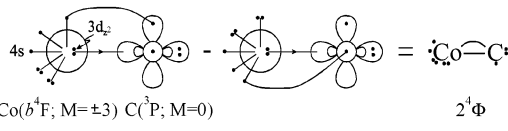
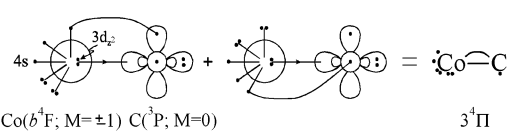
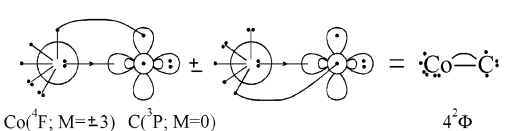
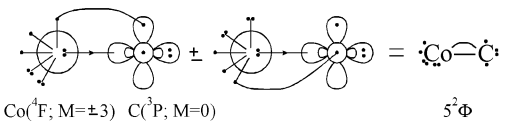
State	Leading Configurations	Population Analysis	vbL	M, M
$X^2\Sigma^+$	$0.85 \left 1\sigma^2 2\sigma^2 3\sigma^1 1\pi_x^2 1\pi_y^2 1\delta_+^2 1\delta_-^2 \right\rangle_{A_1}$	$4s^{1.92} 4p_z^{0.21} 3d_{z^2}^{1.36} 3d_{xz}^{1.22} 4p_x^{0.03} 3d_{yz}^{1.22} 4p_y^{0.03} 3d_{x^2-y^2}^{1.97} 3d_{xy}^{1.97}$ $2s^{1.73} 2p_z^{0.75} 2p_x^{0.75} 2p_y^{0.75}$		0, 0
$1^2\Delta$	$\frac{1}{\sqrt{2}} \left 1\sigma^2 2\sigma^2 3\sigma^2 \left[0.81(1\pi_x^2 1\pi_y^2) - 0.18(1\pi_x^2 2\pi_y^2 + 2\pi_x^2 1\pi_y^2) \right] \times (1\delta_+^2 1\delta_-^1 + 1\delta_+^1 1\delta_-^2) \right\rangle_{A_1+A_2}$	$4s^{1.24} 4p_z^{0.16} 3d_{z^2}^{1.64} 3d_{xz}^{1.36} 4p_x^{0.04} 3d_{yz}^{1.36} 4p_y^{0.04} 3d_{x^2-y^2}^{1.49} 3d_{xy}^{1.49}$ $2s^{1.76} 2p_z^{1.12} 2p_x^{0.60} 2p_y^{0.60}$		±2, 0
$2^4\Phi$	$0.58 \left (1\sigma^2 2\sigma^2 3\sigma^1) (1\pi_x^2 1\pi_y^2 2\pi_x^1 1\delta_+^2 1\delta_-^1 - 1\pi_x^2 2\pi_x^1 1\pi_y^2 1\delta_+^1 1\delta_-^2) \right\rangle_{B_1}$	$4s^{0.92} 4p_z^{0.22} 3d_{z^2}^{1.37} 3d_{xz}^{1.55} 4p_x^{0.07} 3d_{yz}^{1.55} 4p_y^{0.07} 3d_{x^2-y^2}^{1.49} 3d_{xy}^{1.49}$ $2s^{1.73} 2p_z^{0.71} 2p_x^{0.86} 2p_y^{0.86}$		±3, 0
$3^4\Pi$	$0.59 \left (1\sigma^2 2\sigma^2 3\sigma^1) (1\pi_x^2 1\pi_y^2 2\pi_x^1 1\delta_+^2 1\delta_-^1 + 1\pi_x^2 2\pi_x^1 1\pi_y^2 1\delta_+^1 1\delta_-^2) \right\rangle_{B_1}$	$4s^{0.91} 4p_z^{0.22} 3d_{z^2}^{1.39} 3d_{xz}^{1.55} 4p_x^{0.07} 3d_{yz}^{1.55} 4p_y^{0.07} 3d_{x^2-y^2}^{1.49} 3d_{xy}^{1.49}$ $2s^{1.73} 2p_z^{0.71} 2p_x^{0.85} 2p_y^{0.85}$		±2, ∓1
$4^2\Phi$	$\left (1\sigma^2 2\sigma^2 3\sigma^1) \left[0.51(1\pi_x^2 2\pi_x^1 1\pi_y^2 1\delta_+^1 1\delta_-^2) - 0.42(1\pi_x^2 1\pi_y^2 2\pi_x^1 1\delta_+^2 1\delta_-^1) + 0.28(1\pi_x^2 1\pi_y^2 2\pi_x^1 1\delta_+^1 1\delta_-^1) + 0.22(1\pi_x^2 2\pi_x^1 1\pi_y^2 1\delta_+^1 1\delta_-^2) \right] \right\rangle_{g}$	$4s^{0.95} 4p_z^{0.28} 3d_{z^2}^{1.21} 3d_{xz}^{1.59} 4p_x^{0.04} 3d_{yz}^{1.59} 4p_y^{0.04} 3d_{x^2-y^2}^{1.49} 3d_{xy}^{1.49}$ $2s^{1.74} 2p_z^{0.78} 2p_x^{0.85} 2p_y^{0.85}$		±3, 0
$5^2\Phi$	$\left 0.54(1\sigma^2 2\sigma^2 3\sigma^1 1\pi_x^2 2\pi_x^1 1\pi_y^2 1\delta_+^1 1\delta_-^2) + 0.41(1\sigma^2 2\sigma^2 3\sigma^1 1\pi_x^2 1\pi_y^2 2\pi_x^1 1\delta_+^2 1\delta_-^1) + 0.36(1\sigma^2 2\sigma^2 3\sigma^1 1\pi_x^2 1\pi_y^2 2\pi_x^1 1\delta_+^1 1\delta_-^1) - 0.19(1\sigma^2 2\sigma^2 3\sigma^1 1\pi_x^2 2\pi_x^1 1\pi_y^2 1\delta_+^2 1\delta_-^1) \right\rangle_{B_1}$	$4s^{0.99} 4p_z^{0.22} 3d_{z^2}^{1.37} 3d_{xz}^{1.55} 4p_x^{0.05} 3d_{yz}^{1.55} 4p_y^{0.05} 3d_{x^2-y^2}^{1.49} 3d_{xy}^{1.49}$ $2s^{1.69} 2p_z^{0.68} 2p_x^{0.88} 2p_y^{0.88}$		±2, ±1

TABLE 3: (Continued)

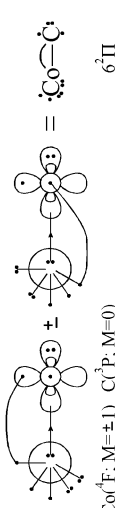
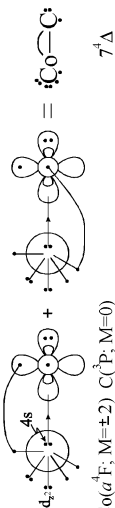
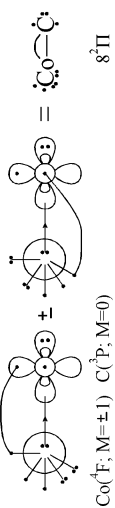
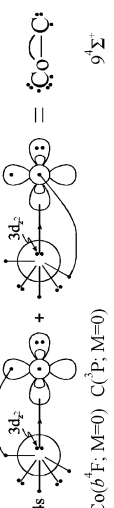
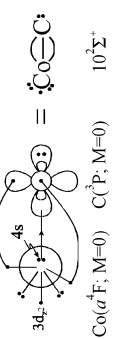
State	Leading Configurations	Population Analysis	vbL	M, M
$6^2\Pi$	$\begin{aligned} & \left[(\sigma^2 2\sigma^2 3\sigma^2) \left[0.43 \left(1\pi_x^2 2\bar{\pi}_x^1 1\pi_y^2 1\delta_+^1 1\delta_-^2 \right) + \right. \right. \\ & + 0.40 \left(1\pi_x^2 1\pi_y^2 2\bar{\pi}_y^1 1\delta_+^1 1\delta_-^1 \right) + 0.21 \left(1\pi_x^2 2\bar{\pi}_x^1 \right. \\ & \left. \left. 1\pi_y^2 1\delta_+^1 1\delta_-^2 \right) + 0.19 \left(1\pi_x^2 2\bar{\pi}_x^1 1\pi_y^2 2\bar{\pi}_y^1 1\delta_+^1 1\delta_-^1 \right) + \right. \\ & \left. + 0.18 \left(1\pi_x^2 1\pi_y^2 2\pi_y^1 1\delta_+^1 1\delta_-^1 \right) \right] + \\ & + 0.22 \left[(\sigma^2 2\sigma^2 3\sigma^2 1\pi_x^2 1\pi_y^2 2\bar{\pi}_y^1 1\delta_+^1 1\delta_-^1) \right]_{B_1} \end{aligned}$	$\begin{aligned} & 4s^{1.00} 4p_z^{0.29} 3d_{z^2}^{1.28} 3d_{xz}^{1.60} 4p_x^{0.04} 3d_{yz}^{1.60} 4p_y^{0.04} 3d_{x^2-y^2}^{1.41} 3d_{xy}^{1.41} \\ & 2s^{1.74} 2p_z^{0.85} 2p_x^{0.85} 2p_y \end{aligned}$	 <p>Co($4F$; $M=\pm 1$) C($3P$; $M=0$) $6^2\Pi$</p>	$\pm 1, 0$
$7^4\Delta$	$\begin{aligned} & \left[(\sigma^2 2\sigma^2 3\sigma^2) \left[0.43 \left(1\pi_x^2 1\pi_y^2 2\pi_y^1 + 1\pi_x^2 2\pi_x^1 1\pi_y^2 \right) \right. \right. \\ & - 0.18 \left(2\pi_x^2 1\pi_y^2 2\pi_y^1 + 1\pi_x^2 2\pi_x^1 2\pi_y^2 \right) \left[1\delta_+^1 1\delta_-^2 + \right. \\ & \left. \left. + 0.40 \left(\sigma^2 2\sigma^2 3\sigma^2 4\sigma^1 1\pi_x^2 1\pi_y^2 1\delta_+^1 1\delta_-^2 \right) \right] \right]_{A_1} \end{aligned}$	$\begin{aligned} & 4s^{1.12} 4p_z^{0.33} 3d_{z^2}^{1.87} 3d_{xz}^{1.14} 4p_x^{0.05} 3d_{yz}^{1.14} 4p_y^{0.05} 3d_{x^2-y^2}^{1.00} 3d_{xy}^{2.00} \\ & 2s^{1.72} 2p_z^{0.88} 2p_x^{0.81} 2p_y^{0.81} \end{aligned}$	 <p>Co($4F$; $M=\pm 2$) C($3P$; $M=0$) $7^4\Delta$</p>	$\pm 2, 0$
$8^2\Pi$	$\begin{aligned} & \left[(\sigma^2 2\sigma^2 3\sigma^2 3\sigma^2 1\pi_x^2 1\pi_y^2 2\pi_y^1 1\delta_+^2 1\delta_-^1) \right. \\ & - 0.52 \left[(\sigma^2 2\sigma^2 3\sigma^2 3\sigma^2 1\pi_x^2 2\pi_x^1 1\pi_y^2 1\delta_+^1 1\delta_-^2) \right. \\ & \left. \left. - 0.17 \left(\sigma^2 2\sigma^2 3\sigma^2 1\pi_x^2 2\pi_x^1 1\pi_y^2 1\delta_+^1 1\delta_-^2 \right) \right] \right]_{B_1} \end{aligned}$	$\begin{aligned} & 4s^{0.99} 4p_z^{0.21} 3d_{z^2}^{1.37} 3d_{xz}^{1.57} 4p_x^{0.06} 3d_{yz}^{1.57} 4p_y^{0.06} 3d_{x^2-y^2}^{1.49} 3d_{xy}^{1.49} \\ & 2s^{1.70} 2p_z^{0.71} 2p_x^{0.86} 2p_y^{0.86} \end{aligned}$	 <p>Co($4F$; $M=\pm 1$) C($3P$; $M=0$) $8^2\Pi$</p>	$\pm 2, \mp 1$
$9^4\Sigma^+$	$\begin{aligned} & \left[(\sigma^2 2\sigma^2 3\sigma^2) \left[0.37 \left(1\pi_x^2 1\pi_y^2 2\pi_y^1 + 1\pi_x^2 2\pi_x^1 1\pi_y^2 \right) \right. \right. \\ & + 0.23 \left(1\pi_x^2 2\bar{\pi}_x^1 1\pi_y^2 2\pi_y^1 \right) + 0.19 \left(1\pi_x^2 2\pi_x^1 1\pi_y^2 2\bar{\pi}_y^1 \right) \left. \right] \\ & 1\delta_+^2 1\delta_-^2 + (\sigma^2 2\sigma^2 3\sigma^2) \left[0.30 \left(1\pi_x^2 2\bar{\pi}_x^1 1\pi_y^2 2\pi_y^1 \right) \right. \\ & + 0.22 \left(1\pi_x^2 2\pi_x^1 1\pi_y^2 2\bar{\pi}_y^1 \right) \left. \right] 1\delta_+^1 1\delta_-^1 \\ & - 0.20 \left(1\pi_x^2 2\pi_x^1 1\pi_y^2 2\pi_y^1 1\delta_+^1 1\delta_-^1 \right) \\ & + 0.20 \left[(\sigma^2 2\sigma^2 3\sigma^2 4\sigma^1 1\pi_x^2 1\pi_y^2 1\delta_+^2 1\delta_-^2) \right]_{A_1} \end{aligned}$	$\begin{aligned} & 4s^{0.97} 4p_z^{0.30} 3d_{z^2}^{1.20} 3d_{xz}^{1.39} 4p_x^{0.05} 3d_{yz}^{1.39} 4p_y^{0.05} 3d_{x^2-y^2}^{1.65} 3d_{xy}^{1.65} \\ & 2s^{1.72} 2p_z^{0.78} 2p_x^{0.88} 2p_y^{0.88} \end{aligned}$	 <p>Co($6F$; $M=0$) C($3P$; $M=0$) $9^4\Sigma^+$</p>	$0, 0$
$10^2\Sigma^+$	$\begin{aligned} & \left[0.31 \left(\sigma^2 2\sigma^2 3\sigma^2 \right) - 0.25 \left(\sigma^2 2\sigma^2 3\sigma^2 4\sigma^1 \right) \right] \\ & \left(1\pi_x^2 1\pi_y^2 1\delta_+^1 1\delta_-^2 \right) + (\sigma^2 2\sigma^2 3\sigma^2) \left[0.30 \left(1\pi_x^2 2\pi_x^1 1\pi_y^2 + \right. \right. \\ & \left. \left. + 1\pi_x^2 1\pi_y^2 2\pi_y^1 \right) - 0.29 \left(1\pi_x^2 1\pi_y^2 \right) \right] 1\delta_+^1 1\delta_-^1 \\ & - 0.19 \left[(\sigma^2 2\sigma^2 3\sigma^2 1\pi_x^2 2\pi_x^1 1\pi_y^2 2\pi_y^1 1\delta_+^2 1\delta_-^2) \right]_{A_1} \end{aligned}$	$\begin{aligned} & 4s^{1.06} 4p_z^{0.23} 3d_{z^2}^{1.23} 3d_{xz}^{1.29} 4p_x^{0.04} 3d_{yz}^{1.29} 4p_y^{0.04} 3d_{x^2-y^2}^{1.79} 3d_{xy}^{1.79} \\ & 2s^{1.67} 2p_z^{0.78} 2p_x^{0.86} 2p_y^{0.86} \end{aligned}$	 <p>Co($4F$; $M=0$) C($3P$; $M=0$) $10^2\Sigma^+$</p>	$\pm 1, \mp 1$

TABLE 3: (Continued)

State	Leading Configurations	Population Analysis	vbL	M, M
$11^2\Delta$	$ \sigma^2 2\sigma^2 3\sigma^1 4\sigma^1 [0.64(\pi_x^2 1\pi_y^2) - 0.19(\pi_x^2 2\pi_y^2) + 2\pi_x^2 1\pi_y^2] (1\delta_x^+ 1\delta_y^2) + 0.36(\sigma^2 2\sigma^2 3\sigma^1 4\sigma^1) 1\pi_x^2 1\pi_y^2 1\delta_x^+ 1\delta_y^2 - 0.18(\sigma^2 2\sigma^2 3\sigma^1 4\sigma^1) (\pi_x^2 1\pi_y^2 2\pi_x^2 + 1\pi_x^2 2\pi_y^2 1\pi_z^2) (1\delta_x^+ 1\delta_y^2) \rangle_A$	$4s^{1.05} 4p_z^{0.38} 3d_{z^2}^{1.82} 3d_{xz}^{1.25} 4p_x^{0.04} 3d_{yz}^{1.50} 4p_y^{0.04} 3d_{x^2-y^2}^{1.50} 3d_{xy}^{1.50}$ $2s^{1.69} 2p_z^{1.00} 2p_x^{0.71} 2p_y^{0.71}$		$\pm 3, \mp 1$
$12^4\Delta$	$0.50 (\sigma^2 2\sigma^2 3\sigma^1 4\sigma^1 1\pi_x^2 1\pi_y^2 1\delta_x^+ 1\delta_y^2) - 0.38 (\sigma^2 2\sigma^2 3\sigma^1 4\sigma^1) (\pi_x^2 2\pi_x^2 1\pi_y^2 + 1\pi_x^2 1\pi_y^2 1\pi_z^2) (1\delta_x^+ 1\delta_y^2) \rangle_A$	$4s^{1.14} 4p_z^{0.33} 3d_{z^2}^{1.68} 3d_{xz}^{1.26} 4p_x^{0.04} 3d_{yz}^{1.98} 4p_y^{0.04} 3d_{x^2-y^2}^{1.98} 3d_{xy}^{1.01}$ $2s^{1.74} 2p_z^{1.05} 2p_x^{0.70} 2p_y^{0.70}$		$\pm 1, \pm 1$
$13^6\Phi$	$ 0.45 (\sigma^2 2\sigma^2 3\sigma^1) (\pi_x^2 2\pi_x^2 1\pi_y^2 2\pi_y^2 1\delta_x^+ 1\delta_y^2) - 1\pi_x^2 2\pi_x^2 1\pi_y^2 2\pi_y^2 1\delta_x^+ 1\delta_y^2 - (\sigma^2 2\sigma^2 3\sigma^1 4\sigma^1) \{ [0.25(\pi_x^2 2\pi_x^2 1\pi_y^2 2\pi_y^2) + 0.19(\pi_x^2 2\pi_x^2 1\pi_y^2 2\pi_y^2)] (1\delta_x^+ 1\delta_y^2) - [0.24(1\pi_x^2 2\pi_x^2 1\pi_y^2 2\pi_y^2) + 0.24(1\pi_x^2 2\pi_x^2 1\pi_y^2 2\pi_y^2)] (1\delta_x^+ 1\delta_y^2) \} + 0.18 (\sigma^2 3\sigma^1 4\sigma^2) (\pi_x^2 2\pi_x^2 1\pi_y^2 2\pi_y^2 1\delta_x^+ 1\delta_y^2 - 1\pi_x^2 2\pi_x^2 1\pi_y^2 2\pi_y^2 1\delta_x^+ 1\delta_y^2) \rangle_B$	$4s^{1.05} 4p_z^{0.33} 3d_{z^2}^{1.09} 3d_{xz}^{1.51} 4p_x^{0.05} 3d_{yz}^{1.51} 4p_y^{0.05} 3d_{x^2-y^2}^{1.49} 3d_{xy}^{1.49}$ $2s^{1.71} 2p_z^{0.80} 2p_x^{0.92} 2p_y^{0.92}$		$\pm 3, 0$
$14^6\Sigma^+G$	$ [0.63 (\sigma^2 2\sigma^2 3\sigma^1) - 0.25 (\sigma^2 3\sigma^1 4\sigma^2)] (\pi_x^2 2\pi_x^2 1\pi_y^2 2\pi_y^2 1\delta_x^+ 1\delta_y^2) + 0.33 (\sigma^2 2\sigma^2 3\sigma^1 1\pi_x^2 2\pi_x^2 1\pi_y^2 2\pi_y^2 1\delta_x^+ 1\delta_y^2) - (\sigma^2 2\sigma^2 3\sigma^1 4\sigma^2) [0.29(1\pi_x^2 2\pi_x^2 1\pi_y^2 2\pi_y^2 1\delta_x^+ 1\delta_y^2) + 0.24(1\pi_x^2 2\pi_x^2 1\pi_y^2 2\pi_y^2 1\delta_x^+ 1\delta_y^2) + 0.19(1\pi_x^2 2\pi_x^2 1\pi_y^2 2\pi_y^2 1\delta_x^+ 1\delta_y^2)] \rangle_A$	$4s^{1.07} 4p_z^{0.31} 3d_{z^2}^{1.07} 3d_{xz}^{1.76} 4p_x^{0.06} 3d_{yz}^{1.76} 4p_y^{0.06} 3d_{x^2-y^2}^{1.74} 3d_{xy}^{1.24}$ $2s^{1.75} 2p_z^{0.78} 2p_x^{0.95} 2p_y^{0.95}$		$0, 0$
$14^6\Sigma^+L$	$ 0.80 (\sigma^2 2\sigma^2 3\sigma^1 1\pi_x^2 2\pi_x^2 1\pi_y^2 2\pi_y^2 1\delta_x^+ 1\delta_y^2) + 0.27 (\sigma^2 2\sigma^2 3\sigma^1 1\pi_x^2 2\pi_x^2 1\pi_y^2 2\pi_y^2 1\delta_x^+ 1\delta_y^2) - 0.19 (\sigma^2 3\sigma^1 4\sigma^2 1\pi_x^2 2\pi_x^2 1\pi_y^2 2\pi_y^2 1\delta_x^+ 1\delta_y^2) \rangle_A$	$4s^{0.95} 4p_z^{0.24} 3d_{z^2}^{1.36} 3d_{xz}^{1.81} 4p_x^{0.13} 3d_{yz}^{1.81} 4p_y^{0.13} 3d_{x^2-y^2}^{1.11} 3d_{xy}^{1.11}$ $2s^{1.71} 2p_z^{0.70} 2p_x^{0.93} 2p_y^{0.93}$		$0, 0$

TABLE 3: (Continued)

State	Leading Configurations	Population Analysis	vbl	M, M
15 ⁴ Π	$[0.39(\sigma^2 2\sigma^2 3\sigma^2 1\pi_x^2 1\pi_y^2 2\pi_x^2 1\delta^+ 1\delta^-) + [0.25(\sigma^2 2\sigma^2 3\sigma^2) + 0.23(\sigma^2 2\sigma^2 3\sigma^2) (1\pi_x^2 1\pi_y^2 2\pi_x^2 1\delta^+ 1\delta^- + 1\pi_x^2 2\pi_x^2 1\pi_y^2 1\delta^+ 1\delta^-)]]_{B_1}$	$4s^{1.14} 4p_z^{0.23} 3d_{z^2}^{1.45} 3d_{xz}^{0.06} 4p_x 3d_{yz}^{1.56} 4p_y 3d_{x^2-y^2}^{1.34} 3d_{xy}^{1.34} 2s^{1.69} 2p_z^{0.78} 2p_x^{0.88} 2p_y$		±1, 0
16 ⁴ Φ	$[0.30(\sigma^2 2\sigma^2 3\sigma^2 (1\pi_x^2 1\pi_y^2 2\pi_x^2 1\delta^+ 1\delta^-) + 1\pi_x^2 2\pi_x^2 1\pi_y^2 1\delta^+ 1\delta^-) - 0.26(\sigma^2 2\sigma^2 3\sigma^2 1\pi_x^2 1\pi_y^2 2\pi_x^2 1\delta^+ 1\delta^-) - 0.20(\sigma^2 2\sigma^2 3\sigma^2 4\sigma^2 1\pi_x^2 2\pi_x^2 1\pi_y^2 1\delta^+ 1\delta^-) - 0.18(\sigma^2 2\sigma^2 3\sigma^2 1\pi_x^2 2\pi_x^2 1\pi_y^2 2\pi_x^2 1\delta^+ 1\delta^-)]_{B_1}$	$4s^{1.10} 4p_z^{0.24} 3d_{z^2}^{1.20} 3d_{xz}^{1.53} 4p_x 3d_{yz}^{1.53} 4p_y 3d_{x^2-y^2}^{1.49} 3d_{xy}^{1.49} 2s^{1.65} 2p_z^{0.77} 2p_x^{0.91} 2p_y^{0.93}$		±2, ±1
17 ⁶ Π	$[0.3(\sigma^2 2\sigma^2 3\sigma^2 1\pi_x^2 2\pi_x^2 1\pi_y^2 2\pi_y^2 1\delta^+ 1\delta^-) + 0.20(\sigma^2 2\sigma^2 3\sigma^2 4\sigma^2 1\pi_x^2 2\pi_x^2 1\pi_y^2 2\pi_y^2 1\delta^+ 1\delta^-) - 0.34(\sigma^2 2\sigma^2 3\sigma^2 (1\pi_x^2 2\pi_x^2 1\pi_y^2 2\pi_y^2 1\delta^+ 1\delta^-) + 1\pi_x^2 2\pi_x^2 1\pi_y^2 2\pi_y^2 1\delta^+ 1\delta^-) - (\sigma^2 2\sigma^2 3\sigma^2 4\sigma^2) + [0.20(\sigma^2 2\pi_x^2 1\pi_y^2 2\pi_y^2 1\delta^+ 1\delta^-) + 1\pi_x^2 2\pi_x^2 1\pi_y^2 2\pi_y^2 1\delta^+ 1\delta^-] + 0.23(1\pi_x^2 2\pi_x^2 1\pi_y^2 2\pi_y^2 1\delta^+ 1\delta^-)] + 0.19(\sigma^2 2\sigma^2 3\sigma^2 (1\pi_x^2 2\pi_x^2 1\pi_y^2 2\pi_y^2 1\delta^+ 1\delta^-) - 1\pi_x^2 2\pi_x^2 1\pi_y^2 2\pi_y^2 1\delta^+ 1\delta^-)]_{B_1}$	$4s^{1.08} 4p_z^{0.33} 3d_{z^2}^{1.34} 3d_{xz}^{1.37} 4p_x 3d_{yz}^{1.66} 4p_y 3d_{x^2-y^2}^{1.34} 3d_{xy}^{1.34} 2s^{1.72} 2p_z^{0.79} 2p_x^{0.92} 2p_y^{0.92}$		±1, 0
18 ⁶ Δ	$[0.60(\sigma^2 2\sigma^2 3\sigma^2) - 0.26(\sigma^2 2\sigma^2 4\sigma^2)] (1\pi_x^2 2\pi_x^2 1\pi_y^2 2\pi_y^2 1\delta^+ 1\delta^-) + (\sigma^2 2\sigma^2 3\sigma^2 4\sigma^2) [0.40(1\pi_x^2 1\pi_y^2 2\pi_x^2 + 1\pi_x^2 2\pi_x^2 1\pi_y^2) - 0.23(1\pi_x^2 2\pi_x^2 2\pi_y^2 + 2\pi_x^2 1\pi_y^2 2\pi_y^2)] 1\delta^+ 1\delta^- - 0.23(1\pi_x^2 2\pi_x^2 1\pi_y^2 2\pi_y^2 1\delta^+ 1\delta^-)]_{A_1}$	$4s^{1.11} 4p_z^{0.34} 3d_{z^2}^{0.95} 3d_{xz}^{1.04} 4p_x 3d_{yz}^{1.04} 4p_y 3d_{x^2-y^2}^{1.00} 3d_{xy}^{1.99} 2s^{1.73} 2p_z^{0.81} 2p_x^{0.91} 2p_y^{0.91}$		±2, 0

$9^4\Sigma^+$. This is a double bonded (σ , π) quartet located 41.7 (42.3) kcal/mol above the X state at the MRCI(+Q) level, showing also strongly multireference character.

C. Sextets: $13^6\Phi$, $14^6\Sigma^+$, $17^6\Pi$, and $18^6\Delta$. All four sextets above display strong multireference character, they are σ -single bonded and the in situ carbon atom finds itself in the $M = 0$ component of its 3P state. In all cases the σ -bond is formed by the transfer of about $0.5 e^-$ from the $4s^2$ Co distribution to the empty $2p_z$ orbital of the C atom. These four sextets lie within an energy range of 5 kcal/mol, reflecting their similar bonding interaction (Figure 5).

The PEC of the $14^6\Sigma^+$ shows a global (G) and a local (L) minimum, the result of an avoided crossing with another (not calculated) $^6\Sigma^+$ state correlating to $\text{Co}(b^4F; M = 0) + \text{C}(^3P; M = 0)$. The barrier height between the G–L minima is 2.34 kcal/mol measured from the G-minimum; Figure 5.

4. Summary and Final Remarks

Employing mainly multireference variational methods (MRCI) combined with quantitative basis sets, we calculated 19 states (8 doublets, 7 quartets, 4 sextets) of the diatomic carbide CoC, spanning an energy range of 2.2 eV. For all states we report full potential energy curves, energetics, the usual spectroscopic parameters, dipole moments calculated as expectation values ($\langle\mu\rangle$) and also by the finite field method (μ_{FF}), and spin–orbit (SO) splittings for the eight lowest states other than states of Σ symmetry. With the exception of the two lower states the generally contracted basis set [7s6p4d3f2g/c_o 5s4p3d2f1g/c] was used; for the $X^2\Sigma^+$ and $1^2\Delta$ states the quadruple- ζ cc-basis set for the Co atom was also employed. In addition, for these two states only, RCCSD(T) calculations have been performed around the equilibrium geometry, whereas semicore correlation effects ($3s^23p^6$ of Co) and scalar relativistic corrections have been taken into account. A summary of our main results follows.

(i) It seems almost certain that the ground state is of $^2\Sigma^+$ symmetry, with a $^2\Delta$ state lying higher by less than 3 kcal/mol. Our best estimate of its $D_e(D_0)$ value is 83(82) kcal/mol at $r_e = 1.541 \text{ \AA}$, 0.02 \AA shorter than the experimental bond length. The calculated $^2\Delta_{5/2} - ^2\Delta_{3/2}$ splitting is 989 cm^{-1} at the MRCI level in good agreement with the experimental one of 952 cm^{-1} .

(ii) All 19 calculated states correlate adiabatically to the ground-state atoms $\text{Co}(a^4F) + \text{C}(^3P)$ and are bound, with binding energies (D_e) ranging from 84.2 ($X^2\Sigma^+$) to 29.4 kcal/mol ($18^6\Delta$) at the MRCI+Q level. The ground state has the shortest bond length of all calculated states with the largest bond length being 2.003 \AA ($18^6\Delta$).

(iii) The doublets are double or triple bonded, the quartets double bonded, and the sextets single bonded. With the exception of the $1^2\Delta$, $11^2\Delta$, and $12^4\Delta$ states, where the in situ $\text{C}(^3P)$ atom interacts with its $M = \pm 1$ component, in the remaining 16 states it finds itself in the $M = 0$ projection. On the other hand, $d_{x^2-y^2}(\delta_+)$ and $d_{xy}(\delta_-)$ electrons do not seem to play any significant role in the binding, being localized on the Co atom. In addition, in all states the metal appears to be Mulliken positively charged with a metal-to-carbon charge transfer of about 0.1 to $0.5 e^-$ depending on the state.

(iv) In accord to previous observations,¹⁸ finite field electric dipole moments (μ_{FF}) are significantly larger than expectation value ones ($\langle\mu\rangle$), by as much as 1 Debye ($X^2\Sigma^+$). We believe that, in general, μ_{FF} values should be trusted more than $\langle\mu\rangle$ ones; therefore, the dipole moment of the CoC $X^2\Sigma^+$ state must be pretty close to 2.0 D.

(v) The T_e 's of the following pairs or groups differ by about 1 mhartree at the MRCI level and obviously their real ordering is probably different, $\{6^2\Pi, 7^4\Delta\}$, $\{10^2\Sigma^+, 11^2\Delta, 12^4\Delta, 13^6\Phi\}$, $\{14^6\Sigma^+, 15^4\Pi, 16^4\Phi\}$, $\{17^6\Pi, 18^6\Delta\}$. The ordering is reversed by adding the zero point energy correction $\Delta\omega_e/2$, only for the pair $\{12^4\Delta, 13^6\Phi\}$.

Acknowledgment. This project is co-funded by the European Social Fund and National Resources-(EPEAEK II) PYTHAGORAS (70/3/7373). A.M. thanks the National and Kapodistrian University of Athens for financial support through its Special Account #70/4/7565 for Basic Research.

References and Notes

- (1) (a) Kalemios, A.; Mavridis, A.; Harrison, J. F. *J. Phys. Chem. A* **2001**, *105*, 755. (b) Kalemios, A.; Mavridis, A. *J. Phys. Chem. A* **2002**, *106*, 3905. (c) Kalemios, A.; Dunning, T. H., Jr.; Mavridis, A. *J. Chem. Phys.* **2005**, *123*, 014301. (d) Kalemios, A.; Dunning, T. H., Jr.; Mavridis, A. *J. Chem. Phys.* **2005**, *123*, 014302. (e) Kalemios, A.; Dunning, T. H., Jr.; Mavridis, A. In press. (f) Tzeli, D.; Mavridis, A. *J. Chem. Phys.* **2002**, *116*, 4901. (g) Tzeli, D.; Mavridis, A. *J. Chem. Phys.* **2003**, *118*, 4984; **2005**, *122*, 056101.
- (2) Harrison, J. F. *Chem. Rev.* **2000**, *100*, 679 and references therein.
- (3) van Zee, R. J.; Bianchini, J. J.; Weltner, W., Jr. *Chem. Phys. Lett.* **1986**, *127*, 314.
- (4) Barnes, M.; Merer, A. J.; Metha, G. F. *J. Chem. Phys.* **1995**, *103*, 8360.
- (5) Adam, A. G.; Peers, J. R. D. *J. Mol. Spectrosc.* **1997**, *181*, 24.
- (6) Brewster, M. A.; Ziurys, L. M. *Astrophys. J.* **2001**, *559*, L163.
- (7) Gutsev, G. L.; Andrews, L.; Bauschlicher, C. W., Jr. *Theor. Chem. Acc.* **2003**, *109*, 298.
- (8) Borin, A. C.; Gobbo, J. P.; Roos, B. O. *Chem. Phys. Lett.* **2006**, *418*, 311.
- (9) Finley, J.; Malmqvist, P.-Å.; Roos, B. O.; Serrano-Andrés, L. *Chem. Phys. Lett.* **1998**, *288*, 299.
- (10) Roos, B. O.; Lindh, R.; Malmqvist, P.-Å.; Veryazov, V.; Widmark, P.-O. *J. Phys. Chem. A* **2005**, *109*, 6575 and references therein.
- (11) Bauschlicher, C. W., Jr. *Theor. Chim. Acta* **1995**, *92*, 183.
- (12) Dunning, T. H., Jr. *J. Chem. Phys.* **1989**, *90*, 1007.
- (13) Balabanov, N. B.; Peterson, K. A. *J. Chem. Phys.* **2005**, *123*, 064107.
- (14) Werner, H.-J.; Knowles, P. J. *J. Chem. Phys.* **1988**, *89*, 5803. Knowles, P. J.; Werner, H.-J. *Chem. Phys. Lett.* **1988**, *145*, 514. Werner, H.-J.; Reinsch, E. A. *J. Chem. Phys.* **1982**, *76*, 3144; Werner, H.-J. *Adv. Chem. Phys.* **1987**, *LXIX*, 1.
- (15) Douglas, M.; Kroll, N. M. *Ann. Phys. N. Y.* **1974**, *82*, 89. Hess, B. A. *Phys. Rev. A* **1985**, *32*, 756. Hess, B. A. *Phys. Rev. A* **1986**, *33*, 3742. Jansen, G.; Hess, B. A. *Phys. Rev. A* **1989**, *39*, 6016.
- (16) Berning, A.; Schweizer, M.; Werner, H.-J.; Knowles, P. J.; Palmieri, P. *Mol. Phys.* **2000**, *98*, 1823.
- (17) Boys, S. F.; Bernardi, F. *Mol. Phys.* **1970**, *19*, 553. Liu, B.; Mclean, A. D. *J. Chem. Phys.* **1973**, *59*, 4557. Jansen, H. B.; Ros, P. *Chem. Phys. Lett.* **1969**, *3*, 140.
- (18) Docken, K.; Hinze, J. *J. Chem. Phys.* **1972**, *57*, 4928. Werner, H.-J.; Meyer, W. *J. Chem. Phys.* **1981**, *74*, 5794.
- (19) Langhoff, S. R.; Davidson, E. R. *Int. J. Quantum Chem.* **1974**, *8*, 61; Blomberg, M. R. A.; Siegbahn, P. E. M. *J. Chem. Phys.* **1983**, *78*, 5682.
- (20) MOLPRO 2002 is a package of ab initio programs written by Werner, H.-J.; Knowles, P. J. with contributions by Amos, R. D.; Bernhardsson, A.; Berning, A.; Celani, P.; Cooper, D. L.; Deegan, M. J. O.; Dobbyn, A. J.; Eckert, F.; Hampel, C.; Hetzer, G.; Korona, T.; Lindh, R.; Lloyd, A. W.; McNikolas, S. J.; Manby, F. R.; Meyer, W.; Mura, M. E.; Nicklass, A.; Palmieri, P.; Pitzer, R.; Rauhut, G.; Schütz, M.; Schumann, U.; Stoll, H.; Stone, A. J.; Tarroni, R.; Thorsteinsson, T.
- (21) Moore, C. E. *Atomic Energy Levels*; NSRDS-NBS Circular No. 35; NBS: Washington, DC, 1971.
- (22) Tzeli, D.; Mavridis, A. Unpublished results.
- (23) Gupta, S. K.; Gingerich, K. A. *J. Chem. Phys.* **1981**, *74*, 3584.
- (24) Brugh, D. J.; Morse, M. D. *J. Chem. Phys.* **1997**, *107*, 9772.
- (25) Brugh, D. J.; Morse, M. D. *J. Chem. Phys.* **2002**, *117*, 10703.